Chemical Geology 532 (2020) 119334

Contents lists available at ScienceDirect

Chemical Geology

journal homepage: www.elsevier.com/locate/chemgeo

Cycles of trace elements and isotopes in the ocean – GEOTRACES and beyond

Distribution of iron in the Western Indian Ocean and the Eastern tropical South pacific: An inter-basin comparison☆

James W. Moffett[a,*], Christopher R. German[b]

[a] University of Southern California, 3616 Trousdale Parkway, Los Angeles, CA, USA
[b] Woods Hole Oceanographic Instituition, Woods Hole MA USA

ARTICLE INFO

Keywords:
Oceans
Iron
Hydrothermal
Margin
Arabian Sea
Peru

ABSTRACT

The Western Indian Ocean (WIO) and Eastern Tropical South Pacific (ETSP) are distinctly different regimes, yet they share several important features. These include a strong upwelling system, a large oxygen minimum zone (OMZ) with active denitrification, a spreading center with extensive hydrothermal activity, and a vast oligotrophic upper water column. Here, we show that the distribution and geochemistry of iron shows remarkable similarities as well. In particular, both basins exhibit large sub-surface plumes of iron derived from sediments underlying the oxygen minimum zones and from hydrothermal sources. Moreover, the behavior of Fe, especially its redox cycling, is remarkably similar in the Arabian Sea and Peruvian oxygen minimum zone, reflecting similar processes associated with the nitrogen cycle in each region. The large Fe plumes under each OMZ are well below the oxygen-free depth, yet they are probably dependent on internal redox cycling and scavenging of Fe within the overlying OMZs. Globally, both the Arabian Sea and Peru margin sediments are hot spots of carbon oxidation, which probably contributes to their importance as Fe sources.

The fate of hydrothermally derived Fe in the WIO and ETSP is particularly interesting to compare because their source terms are very different even though their oxidation rates, once they have entered the water column, should be directly comparable. In the ETSP, hydrothermal inputs from along a section of the ultra-fast spreading Southern East Pacific Rise (SEPR) are integrated into a single coherent plume that is exported west across the ocean interior for > 4000 km. In contrast, hydrothermal inputs to the WIO derive from multiple sources including outflow from the Red Sea via the Gulf of Aden, the Indonesian Throughflow, and from multiple vent-sources along the Carlsbad Ridge, Central Indian Ridge and SW Indian Ridge which are slow, medium and ultra-slow spreading, respectively. As a result, hydrothermally sourced Fe distributions are more complex in the WIO, with several overlapping plumes and distinctly different distributions of two other hydrothermally-derived metals, aluminum and manganese. Here we argue that comparative studies of these basins, with a future emphasis on benthic-water column interactions, will advance knowledge about Fe biogeochemistry and how distributions in the WIO, in particular, are likely to change in the future.

1. Introduction

The distribution, sources and sinks of iron have been studied extensively in the last two decades in sectional surveys and process studies from many nations. Much of this work has been driven by recognition that iron is an important micronutrient for primary production, and that its distribution is governed by the interaction of a variety of complex processes. There has been a particular explosion of data in the last decade as a result of the GEOTRACES program, and Fe is a key parameter in that program. As a result of the accomplishments of GEOTRACES and many other regional and process studies, there is interest in synthesis studies that can compare and contrast the behavior of Fe in different basins to identify key similarities and differences in order to understand fundamental processes. The primary focus of this paper is on the geochemistry of iron in the Western Indian Ocean (WIO) and the unique factors that control its distribution. In developing this overview, we have decided to compare and contrast it with the Eastern Tropical Pacific, a region with remarkable similarities and important differences. This comparison includes a detailed analysis of the similarities and differences between the two upwelling/OMZ regions, and how this

☆ This article is part of a special issue entitled: "Cycles of trace elements and isotopes in the ocean – GEOTRACES and beyond" - edited by Tim M. Conway, Tristan Horner, Yves Plancherel, and Aridane G. González.

* Corresponding author.
E-mail address: jmoffett@usc.edu (J.W. Moffett).

https://doi.org/10.1016/j.chemgeo.2019.119334
Received 6 June 2018; Received in revised form 1 October 2019; Accepted 9 October 2019
Available online 18 November 2019
0009-2541/

might influence offshore transport of Fe. We examine the differences between these two regimes and the eastern boundary regimes in the tropical Atlantic, which have OMZs but where there is no denitrification or complete absence of oxygen. We also intercompare inputs of hydrothermally sourced Fe. Dissolved Fe in deep sea hydrothermal plumes in both the Western Indian and Eastern Tropical South Pacific oceans should be expected to exhibit similar Fe oxidation rates, hence processes of removal (Field and Sherrell, 2000; Statham et al., 2005). However, the diverse range of geologic settings that host hydrothermal activity in the Indian Ocean should be expected to deliver quite distinct hydrothermal source terms throughout this basin compared to the rather monotonous inputs predicted from ultra-fast spreading ridge crests (German et al., 2016a,b).

Indian Ocean data reviewed in this paper were obtained from numerous international cruises. These include expeditions from the US JGOFS Arabian Sea expedition of the 1990s, the Japanese GEOTRACES section GI04 (2009), a series of Indo-US collaborations in 2004 and 2007, and four US-CLIVAR Repeat Hydrography Sections. This is nevertheless a relatively small body of work; in many of these cruises, Fe was a secondary objective, and only the GEOTRACES Section GI04 sampled the entire water column. However, these cruises include some of the most interesting regions of the basin. Eastern Tropical South Pacific data reviewed here represent results of the US GEOTRACES GP16 Section in 2013, a cruise led by one of us (Moffett) within the Peru Upwelling region in 2005 and an extensive series of process studies carried out by German scientists. Only the GEOTRACES cruise led to a full water column section. Cruise tracks for the two GEOTRACES sections are shown in Figs. 1 and 2.

The GEOTRACES cruises resulted in complete water column sections for dissolved Fe and are shown in Figs. 3 and 4. The most striking finding in each section is evidence for plumes of deep water enriched in dissolved Fe (dFe), indicative of hydrothermal input (Nishioka et al., 2013; Vu and Sohrin, 2013; Resing et al., 2015; Fitzsimmons et al., 2017). The second feature common to both sections is a large plume of Fe arising from the continental margin. In both basins, the continental margin plume is significantly deeper than the oxygen minimum zone itself, and spans a broader depth range than the hydrothermal plume. In the absence of a direct connection with a hydrothermal source or reducing regime, the mechanisms leading to the formation of these plumes are still uncertain.

The most significant differences between Fe sections in the two oceans is that in the WIO, there is considerable overlap between the hydrothermal and margin-derived features. In the following sections, we will argue that in part this reflects multiple significant hydrothermal inputs, particularly in the NW Indian Ocean where output from the Gulf of Aden enters close to the continental margin and can merge with non-hydrothermal sources. In contrast, the two plume systems in the ETSP are separated by more than 3000 km of open ocean with low deep water dFe concentrations.

In the following sections, we discuss the geochemistry of iron within the OMZs in the Arabian Sea and ETSP, including redox cycling and sources of Fe. Then, we address Fe transfer from OMZs offshore via the shelf to basin shuttle. We examine how the shuttle contributes to the formation of deep iron plumes in both systems. Subsequently, we examine the role of hydrothermal sources of Fe in both basins and how to unravel the relative importance of hydrothermal and margin sources in areas of overlap, particularly in the WIO.

2. Iron and oxygen minimum zones

The OMZs in the ETSP and WIO have been studied intensively because of their significance in the carbon and nitrogen cycles. The Arabian Sea hosts one of the world's three main oxygen minimum zones (Morrison et al., 1999). The OMZ is coupled with a highly productive upwelling system off the coasts of Oman and Somalia driven by the Southwest Monsoon. Pronounced HNLC conditions arise during the SW Monsoon that have been shown to result from Fe limitation (Moffett et al., 2015), confirming predictions made by Wiggert and Murtugudde (2007). This is a very seasonal feature. During the winter NE monsoon, extensive dust transport to the region (Pease et al., 1998; Tindale and Pease, 1999) results in high surface water concentrations of Fe and Al (Measures and Vink, 1999). During the spring and fall inter-monsoon periods, dust deposition rates are lower than in winter, but there is little biological scavenging of Fe as oligotrophic conditions prevail. Within the suboxic core of the Arabian Sea OMZ, high concentrations of Fe accumulate. Up to half of the dissolved Fe under these conditions is present as Fe(II), which presumably has a long residence time compared with Fe(III). Local maxima in Fe(II) and total dissolved Fe are coincident with the secondary nitrite maxima (Moffett et al., 2007; Kondo and Moffett, 2013; Moffett et al., 2015). This suggests some relationship between Fe redox cycling and denitrification that has yet to be identified. A zonal transect through the Arabian Sea (Moffett et al., 2015) and the meridional GEOTRACES IO4 transect (Kondo and Moffett, 2013) showed that Fe(II) disappeared beyond the perimeter of the OMZ as defined by the absence of oxygen and the secondary nitrite maximum. The disappearance of Fe(II) was associated with a significant decrease in total dissolved Fe.

In the ETSP OMZ, Fe(II) maxima are also coincident with nitrite and extend to the westernmost extrema of the OMZ, until nitrite disappears. Thus, common processes appear to control Fe redox cycling within both OMZs. Given the coincidence with nitrite, Fe(II) is probably associated with anaerobic respiration, perhaps with Fe(III) being utilized as a terminal electron acceptor (Kondo and Moffett, 2015). Fe(III) can also be used as a terminal electron acceptor in microbial respiration, like nitrate, but thermodynamically, the observation is surprising and remains to be fully explained.

The most striking feature of Fe distribution off Peru is the exceedingly high concentration over the Peruvian shelf (Fig. 5). Concentrations generally range from 20 to 50 nM, with some even higher (Bruland et al., 2005: Vedamati et al., 2014; Resing et al., 2015). These concentrations are surprising because there are no strong sources of fluvial Fe to the shelf; indeed, other fluvial derived elements like manganese are low (Vedamati et al., 2015; Resing et al., 2015). Almost all of the shelf Fe is present as Fe(II) below the oxicline, which explains why it does not immediately precipitate.

Scholz et al. (2011) used the term "Fe trapping" to account for the high concentrations of Fe over the Peruvian shelf. In their mechanism, high rates of Fe(II) released from reducing sediments are balanced by high oxidation rates and settling velocities of Fe in the overlying anaerobic waters. Scholz et al. (2016) hypothesized that this was due to Fe(II) oxidation by nitrate and or nitrite via a microbially catalyzed process. Thus, high water column inventories are constantly interchanging with a large benthic inventory of reactive Fe, resulting in the retention or "trapping" of Fe relative to manganese, which oxidizes more slowly, and does not appear to be oxidized by nitrate or nitrite. As a result, Mn is strongly depleted relative to Fe on the Peruvian shelf (Vedamati et al., 2015).

We do not know if Fe trapping occurs on the shelf of the Arabian Sea because no measurements have been reported from within the Indian EEZ. However, Moffett et al. (2015) and Kondo and Moffett (2013) reported strong gradients in Fe(II) and dissolved Fe within the interior of Arabian Sea OMZ in the absence of any oxygen suggesting Fe(II) oxidation by nitrate may occur here. Moreover, Nishioka et al. (2013) reported that about half of the dissolved Fe within the OMZ was colloidal. Some of this Fe may have been in the form of colloidal Fe oxides produced by Fe(II) oxidation.

One significant difference between these systems is that in Peru, the OMZ lies underneath the area of maximum productivity and upwelling along the coast. In the Arabian Sea, the upwelling and productivity and carbon export is greatest on the west side, off the Omani coast (Buesseler et al., 1998), whilst the OMZ lies to the east (Morrison et al., 1999). This is a consequence of greater ventilation in the west with

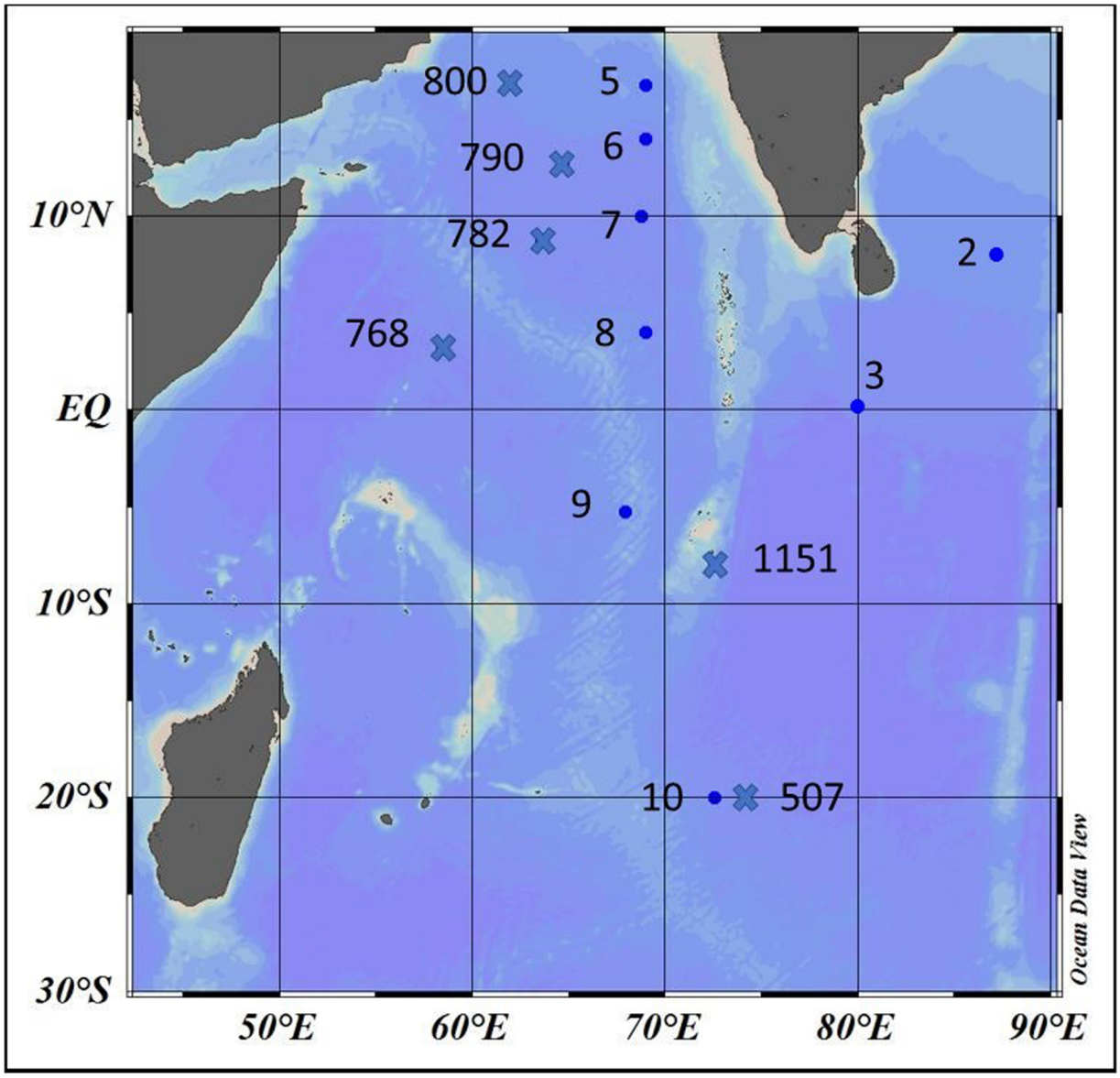

Fig. 1. Station locations for the Japanese GEOTRACES cruise, including two stations in the Bay of Bengal and the GI04 section. From Vu and Sohrin, 2013. WOCE stations, described in Srinivasan et al. (2004) are shown with crosses.

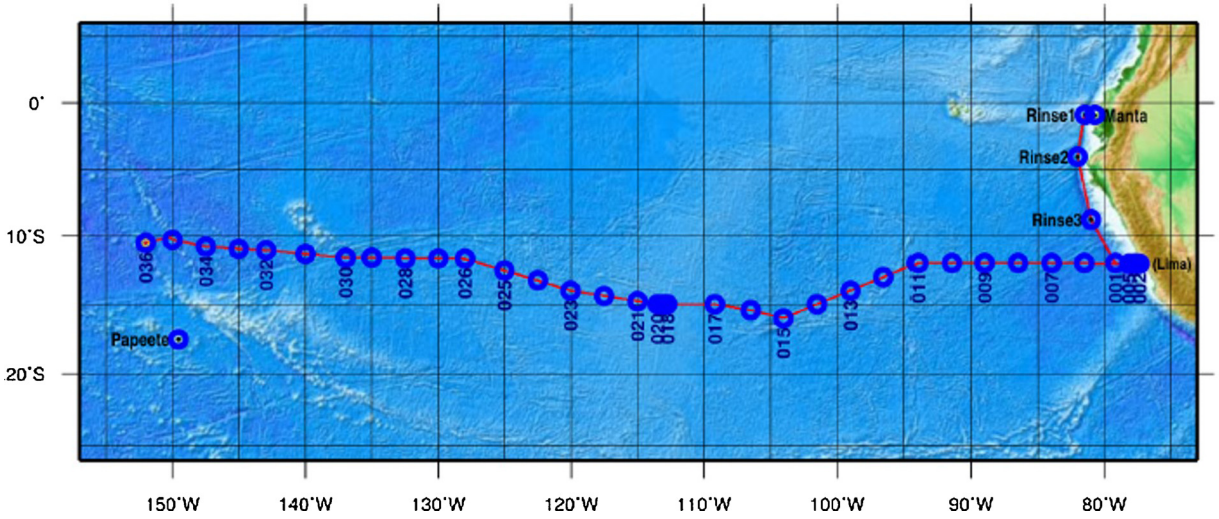

Fig. 2. Station locations for the US GEOTRACES GP 16 Section. Reproduced with permission from Moffett and German, 2018.

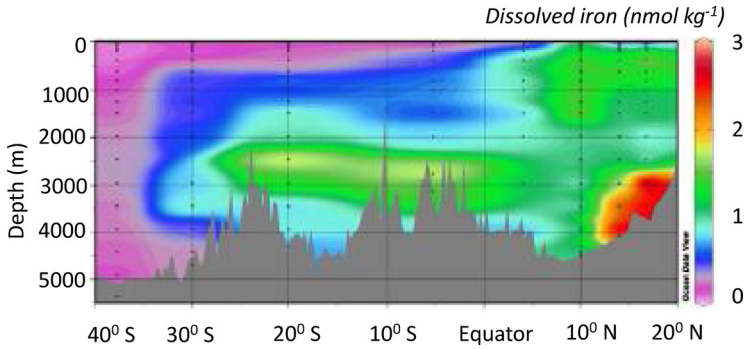

Fig. 3. Section of dissolved iron for GI04. Reproduced with permission from Vu and Sohrin, 2013.

oxygenated waters that counteract oxygen depletion by sinking particles (Olson et al., 1993). As a result, Fe accumulates within the OMZ and is not entrained in the upwelling system. Instead, the principal loss is through advection to the south. This can be seen clearly in a zonal section of dissolved Fe and Fe(II) in the Arabian Sea (Fig. 6; Moffett et al., 2015).

3. Influence of OMZs on Fe distributions offshore

It is important to determine the role of OMZ processes on the transport of Fe to the interior of each basin. Given the very high concentrations of dissolved Fe within OMZs relative to the overlying, oxygenated waters and relative to other oxygenated coastal areas, it might be expected that dissolved Fe would be transported offshore within the OMZ itself, with oxidative scavenging becoming important at the OMZ boundaries. However, this is not the case. Vedamati et al. (2014) reported a strong gradient in dissolved Fe that occurred over the shelf slope break off Peru, without the accompanying appearance of oxygen. In the GP16 cruise, it was revealed that Fe(II) oxidation was associated with the formation of particulate Fe oxides (Heller et al., 2017; Fig. 5), possibly due to the anaerobic oxidation processes hypothesized by Scholz et al., 2016) The oxides reported by Heller et al. (2017) were presumably a product of microbial oxidation on sinking particles.

Not all of the shelf Fe is removed in the vicinity of the shelf slope break. A thin band of Fe(II) extending well offshore (Kondo and Moffett, 2013) is associated with the Equatorial Subsurface Water (ESSW) water mass (Peters et al., 2018). An important goal of the GP16 cruise was to resolve if this feature arises from advection of reduced Fe from the shelf within the OMZ or advection of Fe in surface waters, followed by biological uptake and remineralization at depth.

Results from the US GEOTRACES program utilizing ^{228}Ra and ^{7}Be suggest that the Fe(II) plume arises from advection of Fe(II) from the shelf within the OMZ (Cutter et al., 2018). The model using these two isotopes was tested by iodine measurements. Iodide is enriched in the OMZ, and there is a significant excess concentration over typical seawater values that can only be explained by input from sediments. The model results predicted this outcome, providing confidence that it was also valid for Fe. It is highly likely that the shelf off the west coast of India is also enriched in iron, especially within the region where the OMZ intersects the coast. Excess iodide was observed throughout the Arabian Sea OMZ by Farrenkopf and Luther (2002), who argued that it is derived from benthic sources. If so, then perhaps Fe(II) has an important benthic source as well.

A significant difference between Peru and the Arabian Sea is the input of a massive amount of eolian Fe into the latter during the northeast monsoon, which is almost entirely removed from the upper water column by biological activity during the SW Monsoon (Measures and Vink, 2000). Presumably, much of this Fe is injected into the OMZ by remineralization. By contrast, in the ETSP, aluminum is low in the surface waters (Resing et al., 2017) suggesting that dust inputs are low.

4. Shelf to basin shuttle

The processes discussed so far can be summarized as follows. When the OMZ extends over the shelf, Fe participates in a redox cycle between the sediments and the overlying water. Eventually, this Fe is advected beyond the shelf slope break and sinking Fe oxides settle into deeper waters overlying the continental slope and abyssal plane. This process has been described as the shelf to basin shuttle by previous workers. It is well recognized as an important source of Fe into the interior of the oceans as well as marginal seas like the Baltic (Jilbert and Slomp, 2013; Reed et al., 2016)) in contemporary and ancient oceans. What is the fate of the particulate Fe oxide once it sinks below the OMZ and settles on the seafloor? In the ETSP the GP16 cruise revealed a deep plume off the slope extending down to 3500 m (Fig. 4) that was associated with the Pacific Deep Water water mass (Moffett and German, 2018). Although the overlying water is oxygenated, reducing sediments

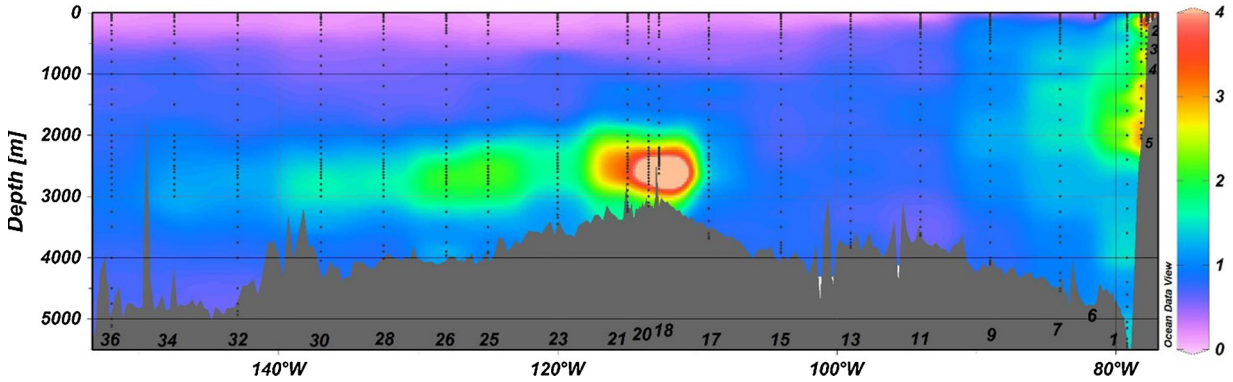

Fig. 4. Section of dissolved Fe for GP16. Reproduced with permission from Resing et al., 2015.

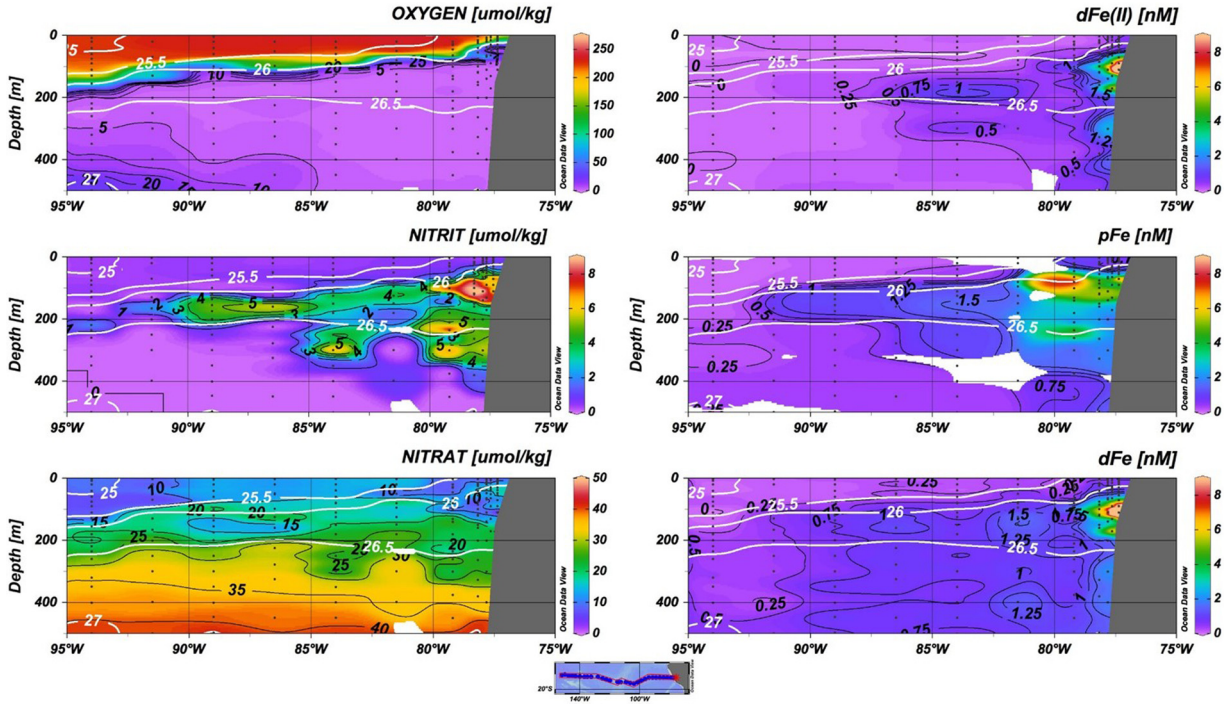

Fig. 5. Nitrate, nitrite, oxygen, dissolved Fe (Fe), particulate Fe (pFe) and Fe(II) for the GP16 stations from within the OMZ. Reproduced with permission from Heller et al., 2017.

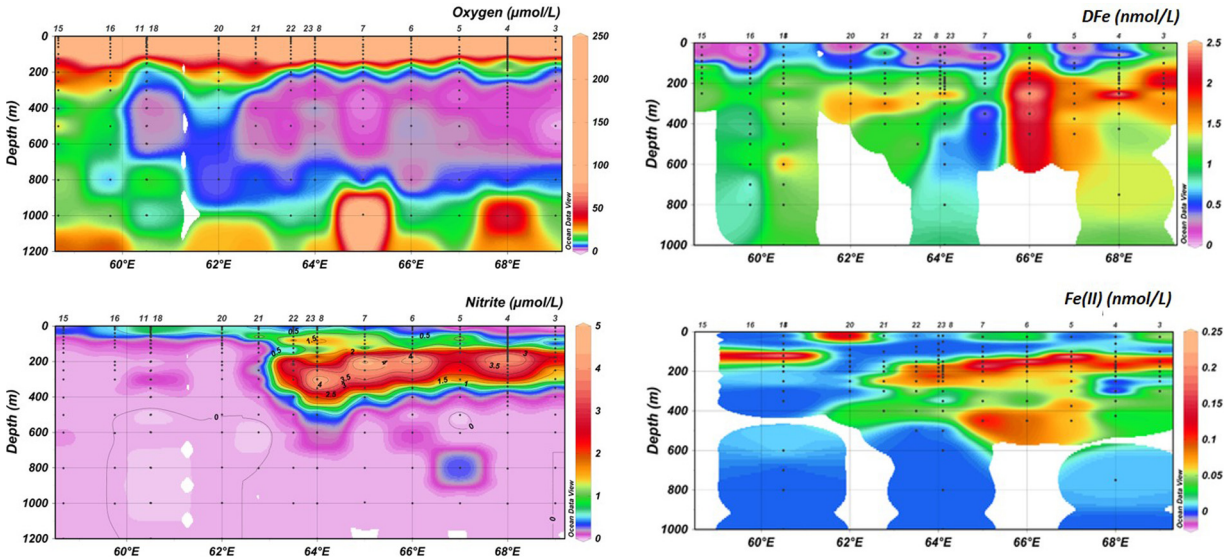

Fig. 6. Nitrite, oxygen, dissolved Fe and Fe(II) from the central Arabian Sea on a zonal section carried out in September 2007. Reproduced with permission from Moffett et al., 2015.

will cause Fe to escape as Fe(II) and then react with organic matter to form soluble Fe(III) complexes. Manganese does not participate in this process because its oxidation kinetics are slow and it is not oxidized by nitrate or nitrite. Thus, it is never removed by oxidative scavenging to waters beneath the OMZ. As a result, neither continental plume contains enriched manganese (Resing et al., 2015; Vu and Sohrin, 2013). One caveat is that the Pacific Deep water flows south (Talley, 2011) and so Fe in the deep plume might not arise exclusively from the overlying OMZ but from regions further north.

The basic features of a plume that arises from the shelf to basin shuttle will be determined by the following factors: (1) Fe supply from the shelf to the OMZ waters beyond the shelf/slope break (2) Seafloor topography and water depth on the slope; (3) Redox conditions in surficial sediments and (4) Ocean currents at the depth horizons of greatest Fe flux as determined by (1)-(3). Off Peru, the plume may be deep because of high fluxes of particulate Fe to sediments in deep water (up to 3000 m). This is partly because of a rapid increase in depth west of the shelf-slope break – associated with the Peru Trench, which reaches depths greater than 6000 m. It also may reflect the importance of westward transport processes, including mesoscale eddies characteristic of the region (Czeschel et al., 2018) that can episodically transport Fe quickly relative to oxidative removal. Callbeck et al. (2018) showed that such eddies are responsible for enhanced rates of sulfide oxidation well beyond the shelf slope break. If rates of Fe removal are comparable to rates of denitrification (a reasonable assumption given the central role of nitrate as an oxidant of Fe(II)) then

such eddies may be very important in Fe transport.

Do similar processes contribute to deep plume features in the WIO? It is difficult to say, because hydrothermal Fe exiting the Gulf of Aden mingles with Fe transported south from the Arabian Sea (see next section). However, the complete absence of any enrichment in Mn and Al north of 10 °N suggests that much of this Fe may be derived from the continental margin. That reasoning is by analogy with the deep Fe plume off Peru, where Mn and Al are exceedingly low (Vu and Sohrin, 2013), in contrast to the hydrothermal plume, where Mn and Al are high (Resing et al., 2015). In the WIO, the deep iron plume features associated with the continental margin exhibit a more complex structure, with a shallow plume between the base of the OMZ and 1500 m, and a deeper plume at > 3000 m. This may reflect Fe sources at different sedimentary horizon but may also be a consequence of prevailing currents. Between 1000 m and 3000 m there are strong zonal currents in this region (Talley, 2011), which, in this section, could be diluting the Fe in the middle of the plume.

. There are other examples of deep Fe plumes arising from continental margins. Saito et al. (2013) reported a large plume of Fe off the Namibian coast. That is interesting because it is also a highly productive region with reducing sediments, but it does not have an extensive zone of active denitrification. Similarly, there is a modest feature off the coast of Senegal, in a region with an oxygen minimum but no water column denitrification, although it is largely confined to the upper 1000 m over the slope (Klar et al., 2018). Thus the sequence of steps that lead to the shelf to basin shuttle may not be absolutely dependent on the absence of oxygen over the shelf. Nevertheless, dFe concentrations over the Peruvian shelf are at least 10x higher than shelf water column concentrations reported off Senegal (Klar et al., 2018) or Namibia (Noble et al., 2012; Saito et al., 2013), so it seems likely that the shelf to basin shuttle is more efficient in Peru. If so, then what takes the place of the oxidative step over the shelf/slope break that would facilitate transport of Fe to the plume depths? It is useful to consider criterion (3), above, the redox state of the sediments and its impact on benthic Fe supply. There are several models that have been published recently that provide useful insight. Dale et al. (2015) provides direct estimates of Fe fluxes from sediments, utilizing estimates of C oxidation rates as a key parameter. Dale et al. (2015) argued that there is a robust relationship between C oxidation and Fe reduction and release, building on Elrod et al. (2004) and incorporated their relationship into their model. Another model developed by Bowles et al. (2014) provides global distributions of sulfate reduction rates in marine sediments but is also based on estimates of C oxidation rates. Most notably, the Bowles et al., 2014 model shows that the two global hot spots for sulfate reduction (and C oxidation and therefore Fe reduction) are the Arabian Sea and Peru upwelling. In particular, a large area of the seafloor in the Arabian Sea is expected to be an important source of Fe. One caveat is that high rates of sulfate reduction might be expected to result in the precipitation of pyrite, substantially lowering Fe fluxes. However Kraal et al. (2012) studied Fe cycling at the sediment water interface in the Arabian Sea and were surprised to find pyrite at only a single location in their large survey. Thus, pyrite formation does not hinder Fe transport and high Fe fluxes over a wide range of depths would contribute to the features observed in Fig. 3.

The other factor to consider is where the Fe comes from to give rise to these plumes. There are strong sources of dust throughout the WIO (Jickells et al., 2005). This is particularly true for the Arabian Sea, which is surrounded by arid lands (grey shaded areas in Fig. 7). However, dusty deposition there is very seasonal. Fig. 7 shows air mass trajectories during the SW monsoon. This feature brings clean air from the open ocean over the region and dust fluxes in the central Arabian Sea during the SW monsoon are low. However, strong NW winds known as the Shamal transport dust from the Arabian Peninsula during this period. They are pushed over the SW monsoonal winds, but precipitation in the eastern Arabian Sea off the Indian coast can result in substantial deposition of this material (Ramaswamy et al., 2017). Measures and Vink (1999) reported high concentrations of aluminum in surface waters of the Arabian Sea, an indicator of dust inputs. Moreover, they estimated that Al deposition was much higher in the eastern Arabian Sea than in the west, and attributed this in part to the precipitation patterns we discussed above. At other times of the year, the SW monsoon does not inhibit dust transport from the Arabian Peninsula. And in winter, the NE monsoon transports dust from important sources in NW India and Pakistan. Cumulatively, there is considerable evidence that these air masses transport substantial material from the Arabian Peninsula to the Arabian Sea (Dahl et al., 2005). Fluvial sources, particularly the Indus River, are important as well, although its sediment load is less than 10% of the Ganges (Milliman and Meade, 1983). Thus, there are strong sources of Fe to the northern and eastern Arabian Sea, the region containing the oxygen minimum zone and also a region of extremely reducing sediments (Kraal et al., 2012).

The sources of Fe to the Eastern Tropical South Pacific are harder to identify. Dust fluxes are small in the region, as indicated by very low concentrations of Al in surface waters on the GP16 transect (Resing et al., 2015). Recent shipboard measurements by Baker et al., 2016a confirm this finding, with elevated dust fluxes primarily over the shelf in the northern region. Moreover, Chever et al.(2015) used Fe isotopic data to argue that dust is only a modest source of Fe to the region. There are no major rivers that discharge into the Peru margin. That does not mean that fluvial inputs are negligible. Scheidegger and Krissek (1982) showed that fluvial inputs to the system are quite large, comparable to fluvial inputs from California. However, they are episodic, with rivers that are dry most of the year transporting large quantities of material offshore during floods.

Regardless of the source, reducing conditions in the sediments lead to large Fe fluxes, confirmed by measurements described previously (Scholz et al., 2011) However, that study also showed that Fe fluxes on the slope (~600 m) decreased drastically. It is not clear if the smaller fluxes are sufficient to supply Fe to the deep plume. However, it is also not clear if the Fe in this plume is derived entirely from the Peru region. The plume is enclosed primarily within the southward flowing Pacific Deep Water (Peters et al., 2018) and has a characteristic, light isotope signature (John et al., 2018) indicative of Fe sourced from a reducing environment. However, that Fe could come from continental margin sources further north off the coast of Ecuador or Colombia, which do have large river inputs, or possibly the Eastern Tropical North Pacific. This uncertainty is in contrast to the WIO, where the continental margin plume clearly arises from the Arabian Sea.

5. Hydrothermal sources of Fe

The plume of Fe spanning the ETSP, as identified on GP16 (Fig. 4), shows that the source of venting is clearly associated with the Southern East Pacific Rise. Lupton and Craig (1981) first established the existence of this single, large and contiguous hydrothermally-sourced plume that extended west across the South Pacific over several thousands of kilometers.. The US GEOTRACES GP16 transect was informed by this work and three further decades of study of the dispersion of this ^{3}He-enriched plume in three dimensions throughout the South Pacific. GP16 results confirmed the plume has remained stable throughout that period (Jenkins et al., 2018). Importantly, the plume is not sourced from a single hydrothermal system, close to where the GP16 transect crossed the SEPR ridge-axis near 15 °S (Moffett and German, 2018). Rather, it reflects the integrated hydrothermal plume output from an extensive section of this ultra-fast spreading ridge axis, ~30 °S to 15 °S that is gathered up by northward topographically-steered currents before being exported west into the ETSP interior. Baker and Urabe (1996) first demonstrated that high concentrations of plume-height hydrothermal material were present all along this section of ultra-fast spreading ridge crest, extending from at least 20 °S. More recently, intercomparison of ^{3}He and ^{14}C data from the GP16 section and earlier WOCE data-sets have provided reinforcing evidence for the

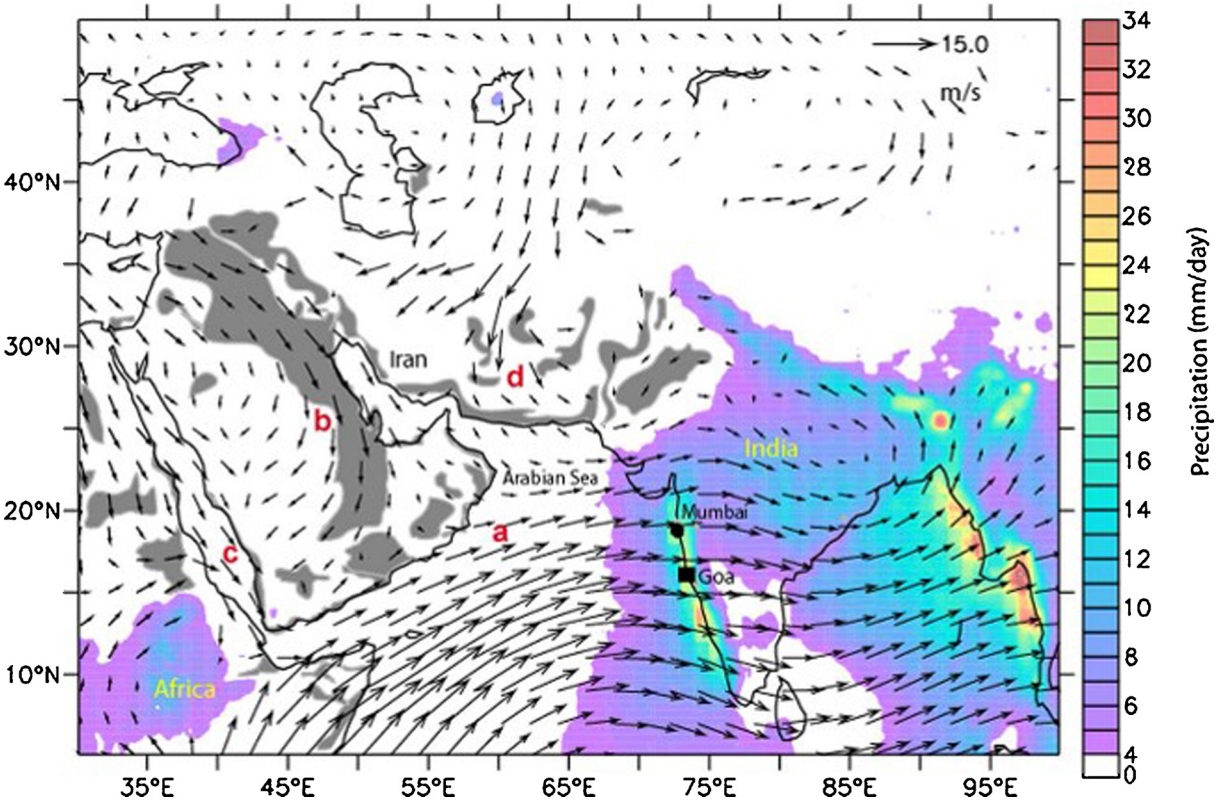

Fig. 7. Quasi-climatology (2003–2014) of the major winds over the northern Indian Ocean during summer monsoon period. The major wind systems are the (a) Low-Level Jet (Findlater Jet), (b) the Shamal winds over the Arabian Peninsula, (c) the Red Sea Winds, and (d) the northerly Levar Winds over SW Asia. Major dust source regions providing mineral dust to the northern Indian Ocean are shown in grey. Reproduced with permission from Ramaswamy et al., 2017.

predominantly northward direction of flow along the SEPR from ~30 °S (Jenkins et al., 2018).

The GEOTRACES GP16 study showed that (a) the dissolved Fe signals measured aboard ship persisted all the way across the remainder of the section, starting at the SEPR ridge crest and extending (at least) as far as the final station occupied at 152 °W and (b) these Fe enrichments were not only accompanied by dissolved Mn and Al anomalies, but also by particulate metal anomalies too (Resing et al., 2015; Fitzsimmons et al., 2017). Further, while Fe/Mn associations in deep ocean hydrothermal plumes are commonplace, measurable Al enrichments at non-buoyant plume height are not (German and Seyfried, 2014). To explain the anomalous enrichment of Al in the SEPR plume, Resing et al. (2015) hypothesized that these enrichments might result from a disproportionately high input of diffuse hydrothermal fluids being entrained into the dispersing 15 °S EPR plume, resulting from volcano-hydrothermal interactions specific to this uniquely fast-spreading section of the global ridge-crest. Anomalously high Al concentrations in end-member hydrothermal vent-fluids have previously been found in direct association with sites of fresh volcanic eruptions in the SW Pacific (Gamo et al., 1993). Intriguingly, in recent work, Baker et al., 2016b have hypothesized that a previously overlooked source of low-temperature hydrothermal inputs may be particularly important to fluxes of water, heat and biogeochemically active species along fast-spreading ridges. Could such material, entrained into the rising buoyant stems of "black smoker" hydrothermal plumes, be responsible for the enhanced enrichment of Al as well as the persistent presence of Fe, Mn, across the GP16 section? Certainly, this could be consistent with a recent modelling study that predicted organic and/or microbial complexation could play an important but previously overlooked role in "fixing" key dissolved (as operationally defined) metals within diffuse flow systems so that they are protected against oxidative precipitation ± scavenging and, instead, be transported long distances in hydrothermal plumes (German et al., 2015).

In the Indian Ocean, the Japanese GEOTRACES GI04 section was meridional and implemented along the same longitude as, and approximately parallel to the N–S orientation of the medium-fast spreading Central Indian Ridge, ~5 °N-25 °S (Fig. 1). This is in contrast to the US GEOTRACES GP16 which was oriented orthogonal to the strike of the SEPR (Fig. 2). Three stations from GI04 were occupied close to the Central Indian Ridge (CIR) axis: station ER8 was occupied at ~5 °N, close to the intersection of the CIR and the slow-spreading Carlsberg Ridge, which tracks NW across the northern Indian Ocean to the Gulf of Aden; stations ER9 and ER10 were also occupied along the strike of the CIR at ~5 °S and 20 °S, with the latter being positioned immediately north of the Rodriguez Triple Junction. Continuing south, the GI04 section also passed close to the SW Indian Ridge (SWIR) at station ER11 before ending in the Crozet basin (ER12).

As shown in Fig. 3, high concentrations of dissolved Fe were observed at all four of these ridge-proximal stations (E8-E11). Importantly, however, detailed analysis of the profiles at each site shows that these anomalies do not form a coherent plume but, rather, occur with varying magnitudes of anomaly and at differing water depths. In the south, highest Fe concentrations at station ER11 are observed at a depth of ~3500 m close to 65 °E, 30 °S. This is very close to where hydrothermal plumes were first reported, between 63.5 °E and 65.5 °E, along the deep SW Indian Ridge – the first vents to be reported along *any* ultra-slow spreading ridge (German et al., 1998). To the north, station ER10 at ~20 °S reveals both the strongest and the shallowest dissolved Fe hydrothermal plume anomalies observed along the GI04 section. Here, maximum dissolved Fe concentrations are observed ~1 km shallower than at ER11, consistent with the faster-spreading (hence, shallower) Central Indian Ridge axis. As with the station ER11 at the SWIR, station ER10 was also occupied close to a location where multiple sites of deep sea hydrothermal plumes had previously been

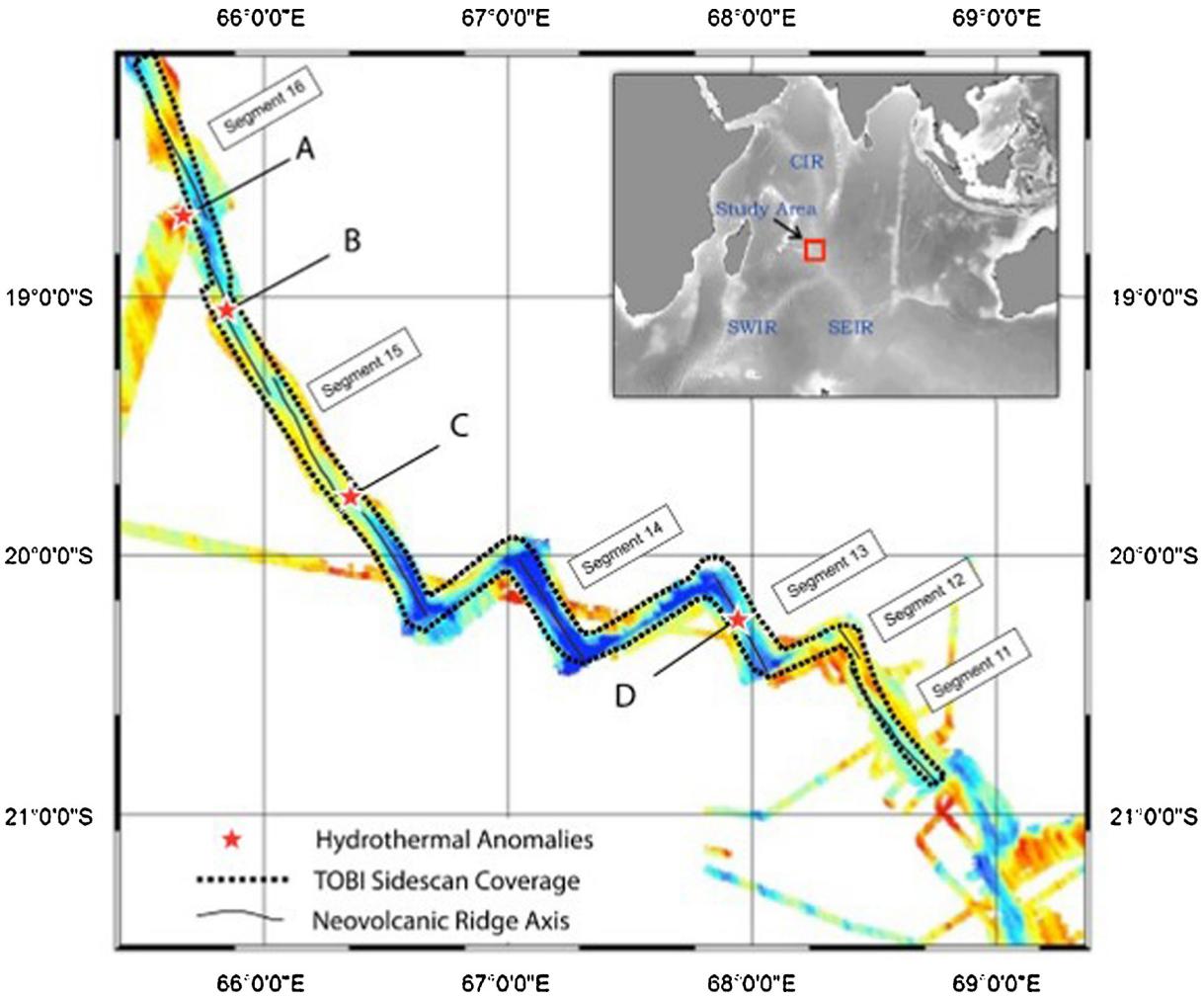

Fig. 8. Evidence for multiple sources of hydrothermal Fe in the vicinity of 20°S from a survey carried out in 2001. Details in the supplementary materials.

detected (Fig. 8) from *in situ* optical back scatter sensors deployed from the deep-towed TOBI instrument (German et al., 2001). Importantly, in the case of the CIR, *in situ* optical anomalies from the deep-tow survey were followed up with CTD casts that confirmed their hydrothermal origin through the detection of plumes with anomalously high total dissolvable Mn (TDMn) concentrations (see Supplementary Information). At 20 °S, the ER10 station also coincides with the latitude of WOCE line I3 which revealed the highest ^{3}He concentration anomalies anywhere in the Indian Ocean, within the resolution of that study (Srinivasan et al., 2004). Further, trace metal enriched plumes have previously been observed overlying the known Kairei (25 °S) and Edmond (23 °S) submarine vent-sites (Gamo et al., 1996; Sands et al., 2012). Continuing north, progressively deeper and lower concentration dissolved Fe anomalies are observed at each of stations ER9 (~2800 m) and ER8 (~3000 m). Given the wide separations between these three sites, (~1500 km and ~1000 km), and the vertical offsets between their plume depths, it is unlikely that these signals derive from a common region of strong hydrothermal input close to 20 °S that both weakens and sinks > 1000 m through the water column as it disperses to the north. Instead, multiple sources are likely since plume compositions at each site show widely differing combinations of Fe, Mn (Fig. 9) and Al concentrations (Vu and Sohrin, 2013, data not shown). At the northernmost CIR site, station ER8 exhibits a much lower Fe:Mn ratio than at ER10 which is the opposite of what might be predicted for a common source and a single dispersing plume. Rather, based on our global understanding of the distribution of seafloor hydrothermal systems (see, e.g., Beaulieu et al., 2015; German et al., 2016b) we would predict ≥ 25 distinct vent-sites along the CIR, in a range of diverse geologic settings with differing vent-fluid compositions. This is consistent with what has previously been reported for the two known vent-sites, Kairei and Edmond sites (Van Dover et al., 2001); the four sites inferred from plume anomalies at 18–20 °S (Fig. 8) also exhibit a combination of tectonically-hosted (A, B) and volcanically-hosted (C, D) venting.

Perhaps most intriguing from the northern part of the GI04 section are the locations at which deep hydrothermal Fe and Mn anomalies are *not* observed. He isotope samples were not collected as part of the Japan GEOTRACES GI04 survey, but depth profiles of Fe and Mn from that section (Vu and Sohrin, 2013) are plotted alongside depth profiles of ^{3}He from nearest adjacent WOCE stations (Srinivasan et al., 2004) in Fig. 9. There are no suitable ^{3}He data for this purpose from the SWIR (ER11) station, but all locations along the CIR (ER10, ER9, ER8) reveal a coincidence of deep-water plume anomalies for each of the tracers under consideration (Fe, Mn & ^{3}He). However, when dissolved Mn concentrations are plotted versus ^{3}He (Fig. 10) only the data from ER-9 and ER10 fall along a coherent mixing line consistent with hydrothermal plume discharge. By contrast, stations ER6 and ER7, occupied closer to the Indian continental margin and distant from the ridge axis also show enrichments in deep-water ^{3}He, but without any associated metal enrichments. The stations are not exactly coincident between cruises (Fig. 1) but TS diagrams for deep waters are nearly identical for each respective station (Supplemental Material). Since there are no nearby ridge axes to these stations, we do not believe that these signals (Figs. 9 and 10) derive from nearby but metal-free vent inputs. Rather,

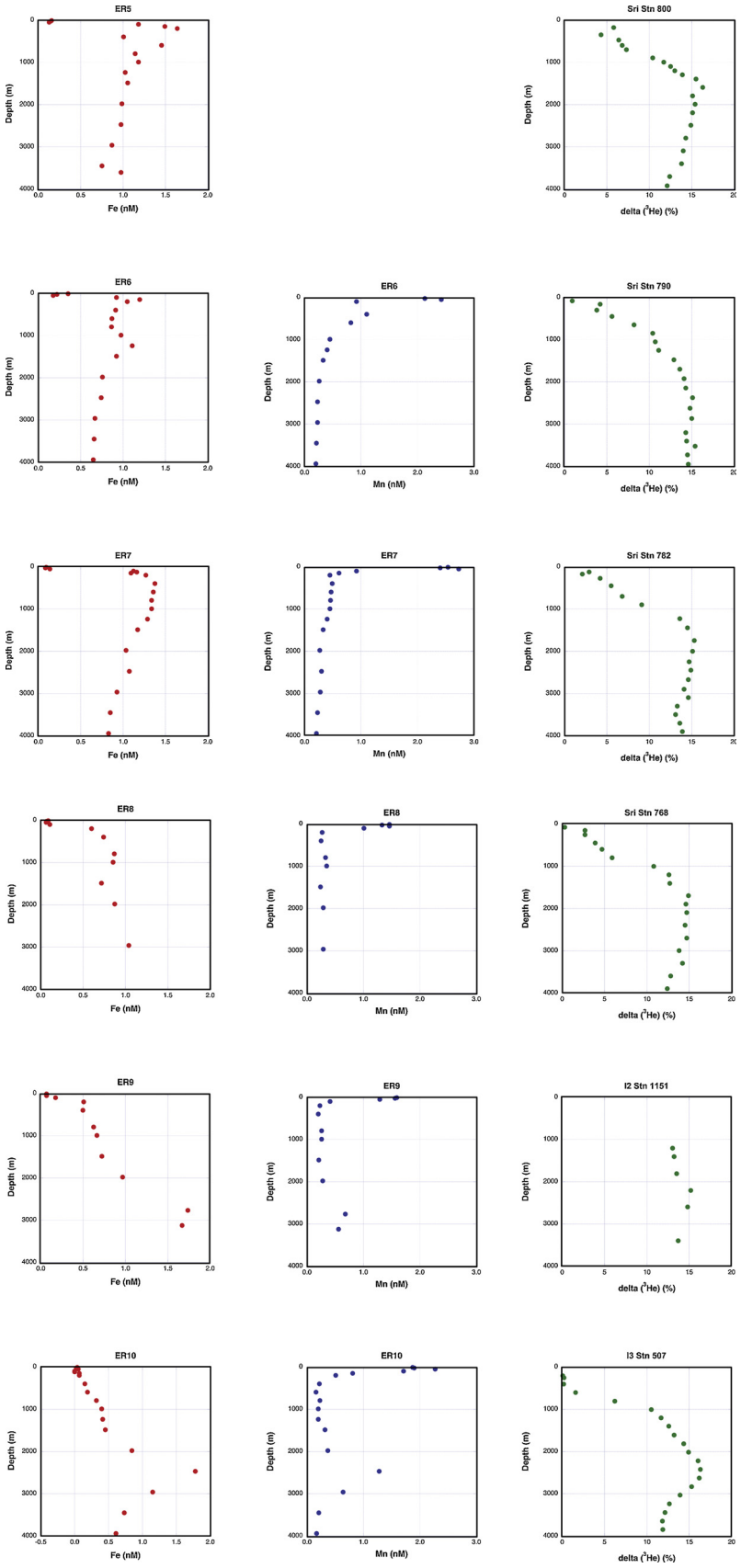

Fig. 9. Depth profiles of ^{3}He, dissolved Fe and dissolved Mn for Japanese GEOTRACES Stas. ER5-ER10, along with WOCE data for ^{3}He from nearby stations.

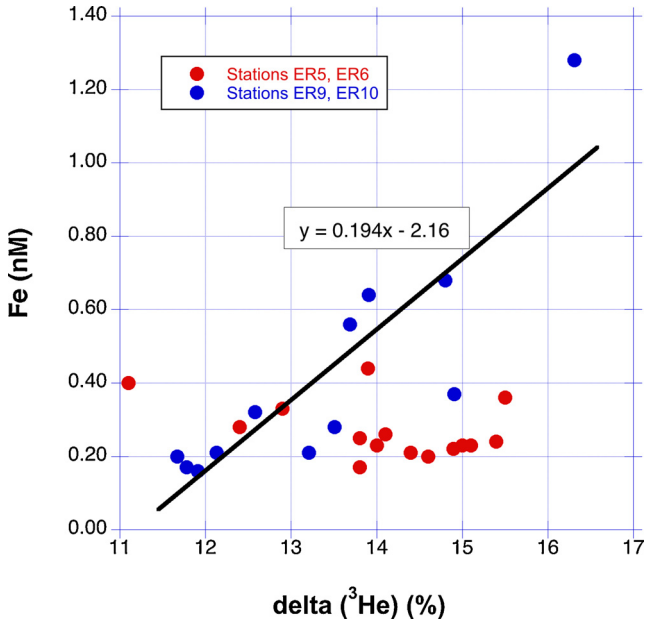

Fig. 10. Plot of dissolved manganese versus 3He for data from Stas. ER9 and ER10 (blue) and Stas. ER6 and ER7 (red).

we propose that these ^{3}He anomalies represent long-range hydrothermal inputs to the NW Indian Ocean from the Gulf of Aden (Srinivasan et al., 2004). Indeed, from an intercomparison of WOCE ^{3}He profiles with Fe and Mn profiles reported by Gamo et al. (2015), rapid separation of ^{3}He from Fe and Mn is readily apparent even within the Gulf of Aden, itself (Gamo et al., 2015; Fig. 8). While profiles of ^{3}He anomalies are relatively constant across the entire IO1 WOCE section at the depth of the deep-water plume (~2000 m), that study showed that dissolved Mn and Fe anomalies decrease rapidly from maxima of ~5 nM and ~15 nM respectively at Station KH-00-5/CTD 7 deep within the Gulf of Aden (12 °N, 47 °E) to values much closer to background at the same depths (< 2 nM Mn, < 5 nM Fe) at Station KH-00-5/CTD 3 closer to the Indian Ocean outflow (13 °N, 49 °E). Given the sluggish nature of clockwise circulation in the NW Indian Ocean, it does not seem unreasonable to infer that the ^{3}He-rich but Fe- and Mn-poor signals seen at similar depths at the far side of the Arabian Sea, at stations ER6 and ER7, represent the distal expression of these same plume inputs, independent of the Fe-rich hydrothermal plume signals derived from the CIR and SWIR to the south.

6. An overview of the Eastern Indian Ocean

A detailed survey of the Eastern Indian Ocean (EIO) is beyond the scope of the paper. However, it is worth noting that one regional sea in the EIO, the Bay of Bengal, has no counterpart in the Pacific. While oxygen is exceedingly low in the Bay of Bengal, oligotrophic conditions in surface waters result in a weak biological pump that does not favor water column denitrification. There were few data for Fe in the region, but that has changed recently with some very thorough and comprehensive surveys by Grand and Measures, participating in the CLIVAR program (Grand et al., 2015a,b,c) and India GEOTRACES Chinni, 2019. Two full water column profiles were measured by the Japanese GEOTRACES group prior to occupying GI04. Their data show that deep water Fe concentrations are lower in the Bay of Bengal than the Arabian Sea (Vu and Sohrin, 2013). Thus, we conclude that the Bay of Bengal is not a significant source of Fe to any of the features in the WIO. The absence of a benthic flux is unsurprising because the Bay of Bengal is highly stratified and oligotrophic, with low C fluxes to the seafloor. Hence Fe reduction rates are expected to be slow.

The EIO hosts no active spreading centers north of the South East Indian Ridge and, hence, has not been subject to hydrothermal exploration in the modern era (Beaulieu et al., 2013; Hein et al., 2016). Rather, Srinivasan et al. (2004), reported that the major source of ^{3}He into the eastern Indian Ocean originated from the hydrothermally active SW Pacific via the Indonesian Throughflow. This same feature also has a significant influence on Si distributions in the EIO and, hence, we identify that a major gap in our existing knowledge is the importance of the Indonesian Throughflow for East Indian Ocean Fe biogeochemistry.

7. Future prognosis

Iron distributions in the Indian Ocean will be strongly affected by climate-induced changes that influence dust and fluvial inputs. These include changes in aridity, monsoon intensity (and its effect on upwelling), air mass trajectories and a variety of processes that influence river flow and sediment load. All of these processes are likely to be most significant in the WIO, which is surrounded by arid land masses and has extreme seasonal variations in climatology. A strengthening SW monsoon, for example, might lead to diminished dust inputs to the Arabian Sea by interfering with dust-laden air masses like the Shamal. However, it is a matter of debate whether the SW Monsoon is increasing or decreasing, and how it might change in the future. There is considerable interest in whether the intensity of the SW Monsoon has changed over the past several decades. Goes et al. (2005) reported that monsoon intensity (estimated by wind speed) increased over the period 1979–2002. However, Izumo et al. (2008) determined from the same data set that the monsoon intensity had actually decreased during this period. Most models predict a strengthening SW monsoon in the future (Wonsick et al., 2014). The intensity of the NE monsoon is predicted to decrease with climate change (Parvathi et al., 2017) which will almost certainly decrease Fe supply to the Arabian Sea.

8. Summary

One reason why the deep Fe plumes in the ETSP and WIO are important is because they may ultimately be a source of Fe to the surface waters in the Southern Ocean, where Fe is thought to limit primary production (Tagliabue et al., 2010). Resing et al. (2015) argued that 15–30% of the primary production below the Southern Polar Front may be sustained by Fe derived from hydrothermal sources. These predictions are preliminary, and require a more detailed assessment of the processes controlling Fe scavenging in the deep ocean. A key assumption is that organic complexation and/or the formation of nanoparticles stabilizes the Fe in hydrothermal plumes with respect to scavenging and removal. Plumes associated with continental margins should receive comparable attention. The plume associated with the Peru Margin is entrained in Pacific Deep Water and flows to the south. The transport of DIC to the Southern Ocean via the same mechanism is already part of a major program (Rosso et al., 2017). The plumes of hydrothermal vs. margin source are very different in their origin and overall transition metal composition, and the latter may have very different Fe speciation characteristics that reflect a reducing sediment source. As such, they warrant a detailed mechanistic study in their own right. Tracking the fate and timescales of plume transport is complicated. General circulation models, the foundation of many biogeochemical Fe models, do not simulate the Fe and ^{3}He plumes in GP16 well (Resing et al., 2015). The fate of the Fe plume extending south from the Arabian Sea is complicated because most currents at those depths are zonal (Talley, 2011) so the abrupt decrease in Fe south of 10 °N above 2000 m may reflect the boundary between two zonal water masses. By contrast, Fe originating from sources between 2000 m and 3500 m may be entrained in the southward flowing Indian Deep Water which is well characterized (e.g. Mantyla and Reid (1995) and references therein). Thus in the WIO, Fe derived from deeper sources may play a more important role than Fe from shallower sources.

One focus of future work should be a detailed study of Fe cycling

processes over the continental shelves of both Peru and the Arabian Sea. In both cases, such work should consider an anticipated strong seasonal variability. For example, important end-member measurements have never been carried out over the Peruvian Shelf during episodic flood events. Iron isotope data have not been made in the WIO. Iron was isotopically much lighter in the Peruvian plume relative to the surrounding waters and the hydrothermal plume. Therefore, iron isotopes may help unravel the relative contribution of the Gulf of Aden hydrothermal system and the Arabian Sea continental margin to the deep Fe plume. The other major focus for future research in the Indian Ocean should be an inter-comparison of trace element and isotope (TEI) cycling across multiple vent systems. Close to the Rodriguez Triple Junction, a variety of distinct seafloor hydrothermal systems are now known, each providing a diversity of source functions into the deep ocean. Importantly, however, these distinct vent inputs are all injected into a common hydrographic regime where redox poise (hence, Fe (II) oxidation rates) should all be directly similar to one another *and* to the oxidation rates for dissolved Fe(II) in the ETSP. This setting provides an ideal natural laboratory, therefore, to tease apart the importance of geologic setting vs oceanographic conditions in regulating the hydrothermal impact on deep ocean Fe biogeochemistry.

Acknowledgements

This research was partially supported by US National Science Foundation grants to James Moffett (OCE-11311731) and Christopher German (OCE-1130870).

Appendix A. Supplementary data

Supplementary material related to this article can be found, in the online version, at doi:https://doi.org/10.1016/j.chemgeo.2019.119334.

References

Baker, A.R., Thomas, M., Bange, H.W., Sanchez, E.P., 2016a. Soluble trace metals in aerosols over the tropical south-east Pacific offshore of Peru. Biogeosciences 13 (3), 817–825.
Baker, E.T., et al., 2016b. How many vent fields? New estimates of vent field populations on ocean ridges from precise mapping of hydrothermal discharge locations. Earth Planet. Sci. Lett. 449, 186–196.
Baker, E.T., Urabe, T., 1996. Extensive distribution of hydrothermal plumes along the superfast spreading East Pacific Rise, 13 degrees 30′-18 degrees 40′S. Journal of Geophysical Research-Solid Earth 101 (B4), 8685–8695.
Beaulieu, S.E., et al., 2013. An authoritative global database for active submarine hydrothermal vent fields. Geochem. Geophys. Geosyst. 14, 4892–4905.
Beaulieu, S.E., Baker, E.T., German, C.R., 2015. Where are the undiscovered hydrothermal vents on oceanic spreading ridges? Deep Sea Res. II 121, 202–212.
Bowles, M.W., Mogollon, J.M., Kasten, S., Zabel, M., Hinrichs, K.U., 2014. Global rates of marine sulfate reduction and implications for sub-sea-floor metabolic activities. Science 344 (6186), 889–891.
Bruland, K.W., Rue, E.L., Smith, G.J., DiTullio, G.R., 2005. Iron, macronutrients and diatom blooms in the Peru upwelling regime: brown and blue waters of Peru. Mar. Chem. 93 (2–4), 81–103.
Buesseler, K., et al., 1998. Upper ocean export of particulate organic carbon in the Arabian Sea derived from thorium-234. Deep-Sea Research Part Ii-Topical Studies in Oceanography 45 (10–11), 2461–2487.
Callbeck, C.M., et al., 2018. Oxygen minimum zone cryptic sulfur cycling sustained by offshore transport of key sulfur oxidizing bacteria. Nat. Commun. 9, 11.
Chever, F., et al., 2015. Total dissolvable and dissolved iron isotopes in the water column of the Peru upwelling regime. Geochim. Cosmochim. Acta 162, 66–82.
Chinni, V., 2019. Spatial variability in dissolved iron concentrations in the marginal and open waters of the Indian Ocean. Marine Chemistry 208, 11–28. https://doi.org/10.1016/j.marchem.2018.11.007.
Cutter, G.A., Moffett, J.W., Nielsdottir, M.C., Sanial, V., 2018. Multiple oxidation state trace elements in suboxic waters off Peru: in situ redox processes and advective/diffusive horizontal transport. Mar. Chem. 201, 77–89.
Czeschel, R., Schutte, F., Weller, R.A., Stramma, L., 2018. Transport, properties, and life cycles of mesoscale eddies in the eastern tropical South Pacific. Ocean. Sci. 14 (4), 731–750.
Dahl, K.A., et al., 2005. Terrigenous plant wax inputs to the Arabian Sea: implications for the reconstruction of winds associated with the Indian Monsoon. Geochim. Cosmochim. Acta 69 (10), 2547–2558.
Dale, A.W., et al., 2015. A revised global estimate of dissolved iron fluxes from marine sediments. Global Biogeochem. Cycles 29 (5), 691–707.
Elrod, V.A., Berelson, W.M., Coale, K.H., Johnson, K.S., 2004. The flux of iron from continental shelf sediments: a missing source for global budgets. Geophys. Res. Lett. 31 (12).
Farrenkopf, A.M., Luther, G.W., 2002. Iodine chemistry reflects productivity and denitrification in the Arabian Sea: evidence for flux of dissolved species from sediments of western India into the OMZ. Deep-Sea Research Part Ii-Topical Studies in Oceanography 49 (12), 2303–2318.
Field, M.P., Sherrell, R.M., 2000. Dissolved and particulate Fe in a hydrothermal plume at 9o45′N, East Pacific Rise: slow Fe(II) oxidation kinetics in Pacific plumes. Geochim. Cosmochim. Acta 64, 619–628.
Fitzsimmons, J.N., et al., 2017. Iron persistence in a distal hydrothermal plume supported by dissolved-particulate exchange. Nat. Geosci. 10 (3), 195–U150.
Gamo, T., et al., 1996. Hydrothermal plumes at the Rodriguez triple junction, Indian ridge. Earth Planet. Sci. Lett. 142 (1–2), 261–270.
Gamo, T., et al., 2015. Hydrothermal plumes in the Gulf of Aden, as characterized by light transmission, Mn, Fe, CH4 and delta C-13-CH4 anomalies. Deep-Sea Research Part Ii-Topical Studies in Oceanography 121, 62–70.
Gamo, T., et al., 1993. Hydrothermal plumes in the Eastern Manus Basin, Bismarck Sea - CH4, Mn, Al and pH anomalies. Deep-Sea Research Part I-Oceanographic Research Papers 40 (1112), 2335–2349.
German, C.R., Baker, E.T., Mevel, C., Tamaki, K., Team, F.S., 1998. Hydrothermal activity along the southwest Indian ridge. Nature 395 (6701), 490–493.
German, C.R., Connelly, D.P., Evans, A.J., Murton, B.J., Curewitz, D., Okino, K., Statham, P.J., Parson, L.M., 2001. Hydrothermal activity along the central indian ridge: ridges, hotspots & philately. EOS Trans. AGU OS42E-06.
German, C.R., Seyfried Jr., W.E., 2014. Hydrothermal processes. In: 2nd ed. In: Holland, H.D., Turekian, K.K. (Eds.), Treatise on GeochemIstry Vol. 8. Elsevier, Oxford, pp. 191–233.
German, C.R., Legendre, L.L., Sander, S.G., Niquil, N., Lebris, N., Luther III, G.W., Bharati, L., Han, X., Le Bris, N., 2015. Hydrothermal Fe cycling and deep ocean organic carbon scavenging: model-based evidence for significant POC supply to seafloor sediments. Earth Planet. Sci. Lett. 419, 143–153.
German, C.R., et al., 2016a. Hydrothermal impacts on trace element and isotope ocean biogeochemistry. Philosophical Transactions of the Royal Society a-Mathematical Physical and Engineering Sciences 374 (2081).
German, C.R., Petersen, S., Hannington, M.D., 2016b. Hydrothermal exploration of mid-ocean ridges: Where might the largest sulfide deposits be forming? Chem. Geol. 420, 114–126.
Goes, J.I., Thoppil, P.G., Gomes, H.D., Fasullo, J.T., 2005. Warming of the Eurasian landmass is making the Arabian Sea more productive. Science 308 (5721), 545–547.
Grand, M.M., et al., 2015a. Dust deposition in the eastern Indian Ocean: the ocean perspective from Antarctica to the Bay of Bengal. Global Biogeochem. Cycles 29 (3), 357–374.
Grand, M.M., et al., 2015b. Dissolved Fe and Al in the upper 1000m of the eastern Indian Ocean: a high-resolution transect along 95 degrees E from the Antarctic margin to the Bay of Bengal. Global Biogeochem. Cycles 29 (3), 375–396.
Grand, M.M., et al., 2015c. The impact of circulation and dust deposition in controlling the distributions of dissolved Fe and Al in the south Indian subtropical gyre. Mar. Chem. 176, 110–125.
Hein, J.R., et al., 2016. Controls on ferromanganese crust composition and reconnaissance resource potential, Ninetyeast Ridge, Indian Ocean. Deep-Sea Research Part I-OceanographicResearch Papers 110, 1–19.
Heller, M.I., et al., 2017. Accumulation of Fe oxyhydroxides in the Peruvian oxygen deficient zone implies non-oxygen dependent Fe oxidation. Geochim. Cosmochim. Acta 211, 174–193.
Izumo, T., et al., 2008. The role of the western arabian sea upwelling in indian monsoon rainfall variability. J. Clim. 21 (21), 5603–5623.
Jenkins, W.J., et al., 2018. The deep distributions of helium isotopes, radiocarbon, and noble gases along the US GEOTRACES East Pacific Zonal Transect (GP16). Mar. Chem. 201, 167–182.
Jickells, T.D., et al., 2005. Global iron connections between desert dust, ocean biogeochemistry, and climate. Science 308 (5718), 67–71.
Jilbert, T., Slomp, C.P., 2013. Iron and manganese shuttles control the formation of authigenic phosphorus minerals in the euxinic basins of the Baltic Sea. Geochim. Cosmochim. Acta 107, 155–169.
John, S.G., et al., 2018. Biogeochemical cycling of Fe and Fe stable isotopes in the eastern tropical south pacific. Mar. Chem. 201, 66–76.
Kraal, P., Slomp, C.P., Reed, D.C., Reichart, G.J., Poulton, S.W., 2012. Sedimentary phosphorus and iron cycling in and below the oxygen minimum zone of the northern Arabian Sea. Biogeosciences 9 (7), 2603–2624.
Klar, J.K., et al., 2018. Sources of dissolved iron to oxygen minimum zone waters on the Senegalese continental margin in the tropical North Atlantic Ocean: Insights from iron isotopes. Geochimica et Cosmochimica Acta 236, 60–78.
Kondo, Y., Moffett, J.W., 2013. Dissolved Fe(II) in the Arabian Sea oxygen minimum zone and western tropical Indian Ocean during the inter-monsoon period. Deep-Sea Research Part I-Oceanographic Research Papers 73, 73–83.
Kondo, Y., Moffett, J.W., 2015. Iron redox cycling and subsurface offshore transport in the eastern tropical South Pacific oxygen minimum zone. Mar. Chem. 168, 95–103.
Lupton, J.E., Craig, H., 1981. A major He-3 source At 15-Degrees-S on the East Pacific Rise. Science 214 (4516), 13–18.
Mantyla, A.W., Reid, J.L., 1995. On the origins of deep and bottom waters of the indian-ocean. Journal of Geophysical Research-Oceans 100 (C2), 2417–2439.
Measures, C.I., Vink, S., 1999. Seasonal variations in the distribution of Fe and Al in the surface waters of the Arabian Sea. Deep-Sea Research Part Ii-Topical Studies in Oceanography 46 (8–9), 1597–1622.

Milliman, J.D., Meade, R.H., 1983. World-wide delivery of river sediment to the oceans. J. Geol. 91 (1), 1–21.
Moffett, J.W., German, C.R., 2018. The USGEOTRACES eastern tropical pacific transect (GP16). Mar. Chem. 201, 1–5.
Moffett, J.W., Goepfert, T.J., Naqvi, S.W.A., 2007. Reduced iron associated with secondary nitrite maxima in the Arabian Sea. Deep-Sea Research Part I-Oceanographic Research Papers 54 (8), 1341–1349.
Moffett, J.W., et al., 2015. Biogeochemistry of iron in the Arabian Sea. Limnol. Oceanogr. 60 (5), 1671–1688.
Morrison, J.M., et al., 1999. The oxygen minimum zone in the Arabian Sea during 1995. Deep-Sea Research Part Ii-Topical Studies in Oceanography 46 (8–9), 1903–1931.
Nishioka, J., Obata, H., Tsumune, D., 2013. Evidence of an extensive spread of hydrothermal dissolved iron in the Indian Ocean. Earth Planet. Sci. Lett. 361, 26–33.
Noble, A.E., et al., 2012. Basin-scale inputs of cobalt, iron, and manganese from the Benguela-Angola front to the South Atlantic Ocean. Limnol. Oceanogr. 57 (4), 989–1010.
Olson, D.B., Hitchcock, G.L., Fine, R.A., Warren, B.A., 1993. Maintenance of the low-oxygen layer in the Central Arabian Sea. Deep-Sea Research Part II-Topical Studies in Oceanography 40 (3), 673–685.
Parvathi, V., Suresh, I., Lengaigne, M., Izumo, T., Vialard, J., 2017. Robust Projected Weakening of Winter Monsoon Winds over the Arabian Sea Under Climate Change. Geophys. Res. Lett. 44 (19), 9833–9843.
Pease, P.P., Tchakerian, V.P., Tindale, N.W., 1998. Aerosols over the Arabian Sea: geochemistry and source areas for Aeolian desert dust. J. Arid Environ. 39 (3), 477–496.
Peters, B.D., et al., 2018. Water mass analysis of the 2013 US GEOTRACES eastern Pacific zonal transect (GP16). Mar. Chem. 201, 6–19.
Ramaswamy, V., Muraleedharan, P.M., Babu, C.P., 2017. Mid-troposphere transport of Middle-East dust over the Arabian Sea and its effect on rainwater composition and sensitive ecosystems over India. Sci. Rep. 7.
Reed, D.C., Gustafsson, B.G., Slomp, C.P., 2016. Shelf-to-basin iron shuttling enhances vivianite formation in deep Baltic Sea sediments. Earth Planet. Sci. Lett. 434, 241–251.
Resing, J.A., et al., 2015. Basin-scale transport of hydrothermal dissolved metals across the South Pacific Ocean. Nature 523 (7559), 200–U140.
Rosso, I., Mazloff, M.R., Verdy, A., Talley, L.D., 2017. Space and time variability of the Southern Ocean carbon budget. Journal of Geophysical Research-Oceans 122 (9), 7407–7432.
Saito, M.A., et al., 2013. Slow-spreading submarine ridges in the South Atlantic as a significant oceanic iron source. Nat. Geosci. 6 (9), 775–779.
Sands, C.M., Connelly, D.P., Statham, P.J., German, C.R., 2012. Size fractionation of trace metals in the Edmond hydrothermal plume, Central Indian Ocean. Earth Planet. Sci. Lett. 319, 15–22.
Scheidegger, K.F., Krissek, L.A., 1982. Dispersal and Deposition of Eolian and Fluvial Sediments off Peru and Northern Chile 93. Geological Society of America Bulletin, pp. 150–162.
Scholz, F., et al., 2011. Early diagenesis of redox-sensitive trace metals in the Peru upwelling area - response to ENSO-related oxygen fluctuations in the water column. Geochim. Cosmochim. Acta 75 (22), 7257–7276.
Scholz, F., et al., 2016. Nitrate-dependent iron oxidation limits iron transport in anoxic ocean regions. Earth Planet. Sci. Lett. 454, 272–281.
Srinivasan, A., et al., 2004. Mantle He-3 distribution and deep circulation in the Indian Ocean. Journal of Geophysical Research-Oceans 109 (C6).
Statham, P.J., German, C.R., Connelly, D.P., 2005. Iron (II) distribution and oxidation kinetics in hydrothermal plumes at the Kairei and Edmond vent sites, Indian Ocean. Earth Planet. Sci. Lett. 236, 588–596.
Tagliabue, A., et al., 2010. Hydrothermal contribution to the oceanic dissolved iron inventory. Nat. Geosci. 3 (4), 252–256.
Talley, L.D., 2011. Descriptive Physical Oceanography: An Introduction, 6th ed. Academic Press 560 pp.
Tindale, N.W., Pease, P.P., 1999. Aerosols over the Arabian Sea: atmospheric transport pathways and concentrations of dust and sea salt. Deep-Sea Research Part Ii-Topical Studies in Oceanography 46 (8–9), 1577–1595.
Van Dover, C.L., et al., 2001. Biogeography and ecological setting of Indian Ocean hydrothermal vents. Science 294 (5543), 818–823.
Vedamati, J., Chan, C., Moffett, J.W., 2015. Distribution of dissolved manganese in the peruvian upwelling and oxygen minimum zone. Geochim. Cosmochim. Acta 156, 222–240.
Vedamati, J., Goepfert, T., Moffett, J.W., 2014. Iron speciation in the eastern tropical South Pacific oxygen minimum zone off Peru. Limnol. Oceanogr. 59 (6), 1945–1957.
Vu, H.T.D., Sohrin, Y., 2013. Diverse stoichiometry of dissolved trace metals in the IndianOcean. Sci. Rep. 3 (1745).
Wiggert, J.D., Murtugudde, R.G., 2007. The sensitivity of the southwest monsoon phytoplankton bloom to variations in aeolian iron deposition over the Arabian Sea. Journal of Geophysical Research-Oceans 112 (C5).
Wonsick, M.M., Pinker, R.T., Ma, Y., 2014. Investigation of the “elevated heat pump” hypothesis of the Asian monsoon using satellite observations. Atmos. Chem. Phys. 14 (16), 8749–8761.